

Functional integration across a gradient of corticostriatal channels controls UP state transitions in the dorsal striatum

Fernando Kasanetz^{*†}, Luis A. Riquelme^{*}, Valeria Della-Maggiore^{*}, Patricio O'Donnell[‡], and M. Gustavo Murer^{*}

^{*}Departamento de Fisiología, Facultad de Medicina, Universidad de Buenos Aires, Paraguay St. 2155 Buenos Aires (C1121ABG), Argentina; and [‡]Departments of Anatomy and Neurobiology and Psychiatry, University of Maryland School of Medicine, 20 Penn St., Room S251, Baltimore, MD 21201

Edited by Ranulfo Romo, Universidad Nacional Autónoma de México, Mexico City, Mexico, and approved April 7, 2008 (received for review November 26, 2007)

Coordinated near-threshold depolarized states in cortical and striatal neurons may contribute to form functionally segregated channels of information processing. Recent anatomical studies have identified pathways that could support spiraling interactions across corticostriatal channels, but a functional outcome of such spiraling remains to be identified. Here, we examined whether plateau depolarizations (UP states) in striatal neurons relate better to active epochs in local field potentials recorded from closely related cortical areas than to those recorded in less-related cortical areas. Our results show that, in anesthetized rats, the coordination between cortical areas and striatal regions obeys a mediolateral gradient and keeps track of slow wave trajectory across the neocortex. Moreover, activity in one cortical area induced phase advances in UP state onset and phase delays in UP state termination in nonmatching striatal regions, reflecting the existence of functional connections that could encode large-scale interactions between corticostriatal channels as subthreshold influences on striatal projection neurons.

basal ganglia | cerebral cortex | *in vivo* intracellular recording | medium spiny neuron | slow waves

The corticostriatal network shows different large-scale dynamics during the wake–sleep cycle. During slow-wave sleep and anesthesia, alternating episodes of strong synaptic activity and membrane potential (V_m) depolarization (UP states) and periods of almost complete silence (DOWN states) spread coordinately across the neocortex every second, bringing up distinctive local field potential (LFP) modulations (1, 2). Subthreshold activity, evidenced either as waves of depolarization over restricted cortical areas or sustained depolarizations, is more intricate during the wake period (2–4). The depolarized states of wakefulness and sleep are an emergent feature of cortical networks (5) and allow online information processing and the reactivation of memory traces during slow-wave sleep (6). Striatal medium spiny neurons (MSNs) also show different depolarized states, the time course of which is linked to cortical activity (7–11), and replay experience-related activity in consonance with the cortex during slow wave sleep (12, 13). Thus, coordinated depolarized states in cortical and striatal neurons support the online and offline operation of corticostriatal circuits.

It has long been thought that corticostriatal pathways are organized in functionally segregated channels (14, 15). This view posits that functional integration occurs “within, rather than between, corticostriatal circuits” (14). However, recent anatomical studies suggest that diffuse corticostriatal projections and multisynaptic circuits linking nonreciprocal cortical and striatal areas could allow interactions across parallel channels (16–20). With the aim of unveiling functional connections between supposedly segregated corticostriatal channels, we examined the timing of UP states in MSNs located in three distinct striatal

regions in relation with LFP in three cortical areas (motor, somatosensory, and cingulate prefrontal cortex) that provide the strongest innervation to those striatal territories. If cross-talk between channels were negligible, the UP states in a given MSN should be strictly coordinated with active states in functionally related cortical areas. Conversely, a high degree of cross-talk would allow one corticostriatal channel to influence active state coordination within other channels. Here, we used the global transitions between active and silent states induced by urethane anesthesia as a tool to investigate whether there are functional connections between corticostriatal channels in the rat.

Results

MSNs were sampled from three territories of the dorsal striatum, rostromedial (IMSN, $n = 22$), caudal (cMSN, $n = 11$), and rostromedial (mMSN, $n = 13$). These territories were chosen to approximately match the projections of the motor, somatosensory, and cingulate cortices, respectively (Fig. 1A; refs. 21–24). All 46 cells displayed the typical electrophysiological features of MSNs (UP states, delayed firing during depolarizing current steps, low input resistance, low firing rate). Those successfully labeled with Neurobiotin exhibited MSN morphological features [see supporting information (SI) Text, Fig. S1, and Table S1].

Slow Waves Are Synchronous Across the Neocortex and Dorsal Striatum in the Urethane-Anesthetized Rat. Slow wave activity (mean frequency: motor cortex = 0.88 ± 0.03 Hz, sensory cortex = 0.9 ± 0.03 Hz, cingulate cortex = 0.83 ± 0.02 Hz) was prevalent in the three cortical areas analyzed (Fig. 1B). To quantify the strength of association between cortical LFPs, we computed coherence, which is an estimate of linear correlation in the frequency domain. Coherence at the main oscillatory frequency was high for any pair of cortical areas (motor sensory = 0.87 ± 0.02 , motor cingulate = 0.86 ± 0.02 , sensory cingulate = 0.88 ± 0.02 ; Figs. 1B and 2A), and phase differences were small and highly variable (sensory motor = $6.72^\circ \pm 19.36$, sensory cingulate = $9.33^\circ \pm 27.12$, motor cingulate = $5.01^\circ \pm 18.91$; mean \pm SD). This is in line with findings in other species and experimental conditions and further suggests that the state of cortical activity induced by urethane resembles closely that observed in quiet wakefulness and natural slow-wave sleep (2–4, 26–28).

UP states in MSNs were coincident with the active part of cortical slow waves (Fig. 1B; Fig. S2), which in our recordings

Author contributions: P.O. and M.G.M. designed research; F.K. performed research; F.K., L.A.R., and V.D.-M. analyzed data; and F.K., P.O., and M.G.M. wrote the paper.

The authors declare no conflict of interest.

This article is a PNAS Direct Submission.

[†]To whom correspondence should be addressed. E-mail: kasanetz@bordeaux.inserm.fr.

This article contains supporting information online at www.pnas.org/cgi/content/full/071113105/DCSupplemental.

© 2008 by The National Academy of Sciences of the USA

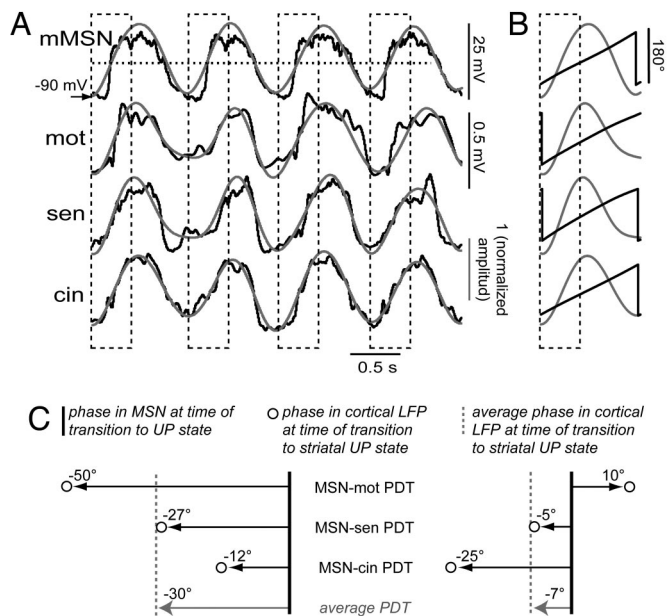


Fig. 2. Phase synchrony analysis. (A) The signals (black) were band-pass wavelet-filtered to obtain waveforms (gray) retaining 0.5- to 2-Hz frequency components describing MSN alternation between UP and DOWN states and cortical slow waves (see also *SI Text* and ref. 11). We defined UP state onsets in the wavelet-filtered V_m as zero crossings (horizontal dotted line) with positive slope and isolated the cortical and striatal counterparts of each slow wave onset (400-ms epochs centered at UP state onset; black dashed boxes). (B) By means of a Hilbert transform, we obtained a continuum of instantaneous phases (saw tooth black line) from each wavelet-filtered signal (gray). (C) Then, for each transition to the UP state, we computed the phase difference between the V_m and each LFP (PDTs; black arrows) and the average phase difference between the V_m and all LFPs (average PDT; gray arrow). Negative PDT indicates that the MSN lags behind cortex. In this example of two UP states of a mMSN, average PDT was higher when the motor cortex was recruited by the slow wave first (Left) than when the cingulate was recruited first (Right). The x-axis is in degrees; values are phase differences. Similar methods were used to estimate PDTs during transitions to the DOWN state (see Fig. S2).

The Trajectory of Active State in Cortex Governs the Timing of Striatal UP States. We speculated further that, if corticostriatal channels were segregated, recruitment of striatal regions by active states propagating through the cortex in different directions should be temporally organized. To assess this possibility, we estimated the average phase difference between MSNs and cortical LFPs at UP state onset (Fig. 2C) for the same time series. This provided one collection of “average PDTs” per MSN, comprising UP states where the “matching” LFP could have either led or lagged behind the other LFPs. Note that the average PDT is an index of the timing of striatal UP states in relation to the average time of cortical activation. We expected average PDTs to be shorter when the matching cortical area led the slow wave, because connected MSNs should have been in the UP state by the time the wave front invaded distant cortical areas (Fig. 2C). This was assessed by classifying average PDTs in three groups, according to the region of the cortex that was leading activity in the striatal regions (Fig. 4A). Reliable patterns of activation of the different striatal regions during slow waves led by the motor, sensory, and cingulate LFPs were identified by using PLS (Fig. 4B; Fig. S3). The average PDT was shorter in the rostralateral striatum and longer in the medial striatum when slow waves were led by the motor cortex, and the opposite pattern was seen for waves led by the cingulate cortex (Fig. 4A and B). Further comparisons within each striatal region confirmed that MSNs reached the UP state sooner during slow waves led by the matching LFP (Fig. 4C). Linear regressions computed for the whole sample of MSNs

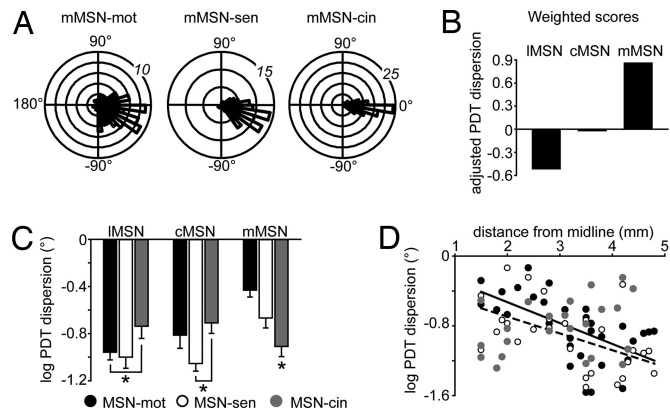


Fig. 3. Graded influence of the motor cortex across the striatum. (A) Circular plots illustrating the rate of occurrence of PDTs along 90 transitions to the UP state for the mMSN depicted in Fig. 1 (italics, calibration of the radial axis). PDTs were more narrowly distributed for the cingulate (cin) than the motor (mot) and sensory (sen) LFPs. (B) Singular profile resulting from the PLS analysis of PDT dispersion. The singular profile represents the contribution of each experimental condition to the observed spatial pattern (see *SI Text* and ref. 51). Here, it shows the nature of the functional association between striatal regions and the motor cortex LFP as assessed from PDT dispersion datasets [lower PDT dispersion in the rostralateral striatum (IMSNs) and higher PDT dispersion in the medial striatum (mMSNs)] and was highly reliable as assessed with permutation tests ($P < 0.0001$). (C) PDT dispersions were next compared within each MSN category. One-way repeated-measures ANOVAs revealed preferential associations (less dispersion) of IMSNs and cMSNs with motor and sensory cortices ($*, P < 0.01$ vs. cingulate; post hoc Holm Sidak test) and of mMSNs with cingulate cortex ($*, P < 0.01$ vs. either motor or sensory). (D) There was a linear relationship between MSN location across the coronal plane (distance from midline) and PDT circular dispersion with motor cortex (black line, regression ANOVA, $P < 0.001$, $r = 0.60$) and sensory cortex LFPs (dashed line, regression ANOVA, $P < 0.005$, $r = 0.52$).

confirmed graded effects of the leading cortical area on UP state onset across the mediolateral axis (Fig. 4D).

Activity in Nonmatching Cortical Areas Modulates Phase Relationships Between a MSN and Its Matching Cortex. Although the data support a mediolateral organization in corticostriatal information flow, none of the findings mentioned above rule out the possibility of cross-talk between corticostriatal channels. Yet, this can be easily inferred based on our data. Cross-talk should not change the PDT between an MSN and its matching LFP when the matching LFP leads (Fig. 5A Upper), because nonmatching cortical areas would activate too late to contribute to UP state onset in the MSN. However, if a slow wave recruits nonmatching cortex first (Fig. 5B Lower), cross-talk would contribute to driving the MSN into the UP state, thus reducing its PDT with the matching LFP. Our results support the existence of cross-talk; for any subset of MSNs, the PDT with the matching LFP was shorter when a nonmatching LFP was recruited first by a slow wave (Fig. 5B).

To establish whether cross-talk operates beyond UP state onset is more difficult. Hypothetically, if the matching cortex enters into the DOWN state while cross-talk influences from nonmatching areas are active, cross-talk inputs would extend the striatal UP state relative to its matching LFP. In fact, this was the case: MSNs reached the DOWN state later in those waves where the matching cortical area was ahead of the nonmatching ones (Fig. 5C). Last, we examined the temporal organization of cross-talk, which, despite the alternating patterns of cortical LFP leading, remained steady overall (Fig. S5). Thus, the analyses are consistent with interactions among separate channels of corticostriatal information processing.

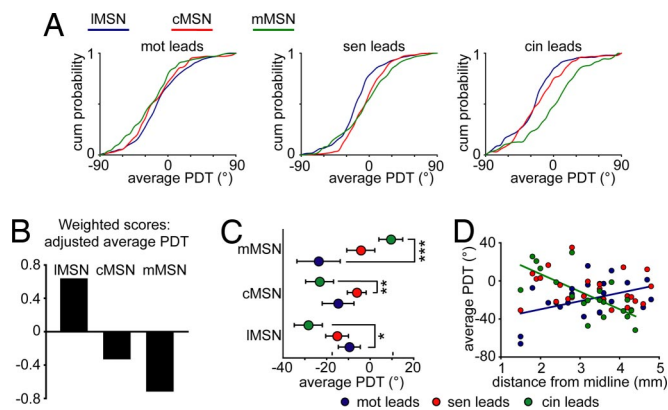


Fig. 4. Vertical propagation of the slow wave. (A) Cumulative frequency histograms showing the average PDTs corresponding to all transitions to the UP state in all MSNs, sorted according to the LFP that had the leading phase (mot leads, sen leads, cin leads). (B) Singular profile ($P < 0.002$) depicting a linear trend for average PDT across striatal regions. The pattern in the singular profile correlated positively with average PDT when the motor cortex led the wave (UP state onset occurred sooner in the rostralateral striatum and later in the medial striatum during these waves) and negatively when the cingulate or the somatosensory cortices were ahead (the medial striatum reached sooner, the rostralateral striatum later, during the UP state; see also Fig. S3). (C) Further comparisons within MSN category show that IMSNs were activated earlier when the motor cortex led ($*, P < 0.01$ vs. cingulate, post hoc Holm Sidak), cMSNs when sensory cortex led ($*, P < 0.01$ vs. cingulate) and mMSNs when cingulate cortex led ($*, P < 0.001$ vs. motor, post hoc Holm Sidak). (D) There was an inverse linear relationship between average PDT and MSN distance from midline when the cingulate LFP led (regression ANOVA, $P < 0.001$, $r = 0.71$) and, conversely, a direct linear relationship when the motor cortex led (regression ANOVA, $P < 0.03$, $r = 0.43$).

Discussion

The striatum is often perceived as an essential component of parallel loops stemming from different cortical areas. This view is based on studies revealing finely ordered motor cortex projections to the striatum (23, 29) and a somatotopic organization of neuronal activity within the motor striatum comparable to that of the motor cortex (14, 30). Parallel studies have reported topographically ordered projections of nonmotor cortical areas to medial regions of the striatum (22, 31–33) and coactivation of these cortical areas and their striatal counterparts during cognitive tasks (34–37). There is also strong evidence of composite encoding of sensorimotor, cognitive, and reward-related information by single neurons widely distributed through the striatum (38–43) and of anatomical pathways that could allow interactions across channels (17–20). Several issues remain controversial or unsolved, such as whether large-scale functional interactions between corticostriatal channels actually occur, their nature (symmetrical or spiraling), and whether the model of corticostriatal segregation can be extended to offline modes of information processing. Here, we provided evidence that corticostriatal segregation and large-scale reciprocal interactions are embedded within the UP states of MSNs in the urethane-anesthetized rat.

Overall, we found there are preferred functional connections that bind cortical areas and striatal regions in coordinated active states. These functional connections approximately define corticostriatal channels. Nevertheless, the striatal regions differed markedly in their degree of selectivity for cortical inputs, and functional coupling, in particular the strength of association with the motor cortex, changed smoothly across the mediolateral axis. The latter finding is consistent with the view that cortical, thalamic, and limbic inputs are organized according to a mediolateral gradient across the dorsal striatum (18, 20). However, that we saw a gradient for only one cortical input suggests other

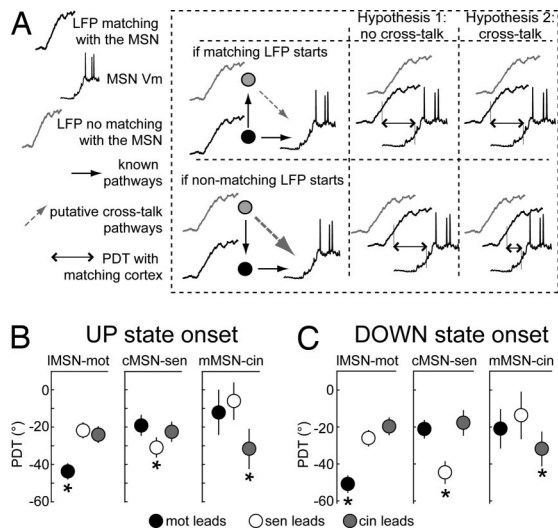


Fig. 5. Functional interactions between corticostriatal channels. (A) Drawings depicting predictions about how the PDT between a MSN and its matching LFP should change depending on the trajectory of the slow wave and whether there is cross-talk. Cross-talk should not change the PDT between a MSN and its matching LFP when the matching LFP leads (Upper), because nonmatching cortical areas would activate too late to contribute to UP state onset in the MSN. However, if a slow wave recruits nonmatching cortex first (Lower), cross-talk would contribute to impelling MSNs into the UP state, thus reducing their PDT with the matching LFP. Circles represent matching (black) and nonmatching (gray) cortical areas; black arrows represent main directions of propagation; and gray arrows, additional putative directions of propagation (cross-talk). (B) Within any group of MSNs, waves recruiting first a nonmatching cortical area reduced the PDT between MSNs and matching LFPs ($*, P < 0.001$, post hoc Holm Sidak test for any comparison between matching and nonmatching, after significant one-way repeated-measure ANOVAs). (C) Predictions can also be drawn about how cross-talk would affect transitions to the DOWN state in MSNs. These transitions should be delayed when the matching LFP turns off first, because the cortex that remains active would spread influences over nonmatching striatal regions and extend the UP state. Indeed, transitions to the DOWN state were delayed in all MSNs when the matching cortex led the transition ($*, P < 0.05$, statistics as above).

channels could follow a different functional architecture. Certainly, our findings fit better with the view that each striatal region shows a particular pattern of connectivity with the three cortical regions analyzed, rather than the view of strictly segregated corticostriatal connections.

Perhaps the strongest evidence for segregation comes from the dynamics of slow waves. When a slow wave spreads from the motor cortex, the rostralateral striatum is enabled before the medial striatum, and the inverse pattern is shown when the cingulate cortex leads the wave. This indicates that functional connections organize the vertical spreading of slow waves according to the preferred mediolateral gradient. Recording UP states simultaneously in several MSNs could provide further confirmation of this view. The only available study of this kind (44) has reported simultaneous UP states in neighboring MSNs. However, timing was assessed from cross-correlations instead of by examining delays according to the direction of active-state propagation in the cortex. Another study assessing functional topography between ventral striatal regions and hippocampal field potentials revealed a gradient in the cross-correlation along several axes but clearest along the mediolateral axis (8). Thus, the mediolateral axis is the strongest organization of corticostriatal connectivity.

We favor the view that the influence of a cortical area is maximal over a striatal region (probably the region receiving the focal projections) but reaches distant regions with an influence that decreases with distance (perhaps through diffuse projec-

tions; see ref. 19). This implies that a given cortical area may influence UP states in striatal regions that relate better to other cortical areas. We demonstrated functional connections across channels by showing that the phase relationship between a MSN and its matching cortical area can be predicted from the timing of the slow wave in nonmatching cortical areas. Our approach to identify cross-talk was inspired by the idea that causality can be inferred from signal interactions “in terms of the predictability of a signal using the knowledge of the immediate past of other signals” (45). To be more precise, we found that, regardless of its site of origin, the front of the traveling wave accelerates UP state onset in nonmatching striatal regions. Thus, it seems that cross-talk influences can operate symmetrically, from sensorimotor to cognitive and from cognitive to sensorimotor channels, depending on the site of initiation of the slow wave. Certainly, mechanisms other than the diffuse corticostriatal projections could support cross-talk, like spiraling loops involving the substantia nigra and thalamus (17). It remains to be determined whether the nucleus accumbens and dorsal striatum are activated coordinately and interact symmetrically or asymmetrically during active states.

Our findings are particularly relevant for slow-wave sleep, because of its resemblance with the global condition induced by urethane (2, 10). They reinforce novel views of slow waves as a global process spreading beyond the thalamocortical system in expanding loops (9, 46, 47). They also strengthen the view that the dynamics of depolarizing states in the striatum, which lacks an intrinsic excitatory driving force, depend highly on the dynamics of cortical networks (8–11). Moreover, the cross-talk influences embedded in the spontaneous activity of MSNs could make MSN responses to specific inputs contingent on associational contexts and modulate corticostriatal synaptic plasticity. This is important, because the striatum is involved in offline processing of memory traces in concert with the cortex (12, 13), and learning has local effects on cortical slow-wave activity (48). In addition, it cannot be ruled out that the functional connections unveiled here operate during wakefulness, for example, shaping the activity in corticostriatal circuits as depolarizing waves travel across the sensorimotor cortex of awake rodents (3, 4). The finding that the transition to the DOWN state in MSNs is delayed when nonmatching cortical areas remain active after the matching one turned off indicates that cross-talk operates beyond active-state onset, perhaps throughout the UP state, leaving open the possibility of a more general role during persistent depolarizations like those seen during attentive behavior. Thus, cross-talk influences could be an integral feature of the network depolarized state, which could be difficult to detect except during global transitions between active and silent states. This is worth considering given the very similar network dynamics that underlie the depolarized states of waking and sleep (5).

In conclusion, we describe a mechanism for the cross-encoding of cortical inputs as subthreshold influences on the depolarized state of MSNs, which could be dynamically shaped during the propagation of depolarization waves through the neocortex. This

endows corticostriatal circuits with integration and segregation capabilities that could be modulated in vigilance- (49) or behavioral-state-dependent manners.

Materials and Methods

Animals, Recordings, and Histology. All methods were similar to those described in Kasanetz *et al.* (9, 11) and are described in more detail in the *SI Text*. Adult male Sprague–Dawley rats ($n = 46$) were used and cared for in accordance with local institutional regulations on the use of laboratory animals (Servicio Nacional de Sanidad y Calidad Agroalimentaria, RS 617/2002, Argentina). Briefly, three concentric bipolar electrodes (SNE-100, Better Hospital Equipment) were used to obtain differential LFP recordings (0.1–300 Hz) from the anterior cingulate/prelimbic (cin), motor (mot), and somatosensory (sen) cortices (Fig. 1A). Intracellular recordings were obtained from rostralateral, rostromedial, and caudal striatum, ipsilateral to LFP recordings (Fig. 1C). Thirty-five MSN recording sites were determined after localizing neurobiotin-labeled neurons or the track left by electrodes in Nissl-stained sections. Eleven additional MSNs recorded in the lateral, medial, or caudal striatal region, as assessed from stereotaxic coordinates, were not used for correlation analyses concerning the exact lateral position (Figs. 1D2, 3C, and 4C).

Signal Analysis. Briefly, functional connectivity was assessed from recordings >90 s. A single coherence spectrum per pair of signals was calculated from the average cross-spectral density normalized by the average spectral density of each signal. To compare coherence among MSN-LFP pairs, a single value of coherence per spectrum was obtained by averaging across the frequency range where cross-spectral power reached significance (values exceeding percentile 95 of the distribution). To isolate individual active states, we extracted the low-frequency components (0.5–2 Hz) of all signals by using a finite impulse response digital filter approximation of the Meyer wavelet function. Transitions to the UP state were detected as zero crossing with a positive slope in the normalized (-1 to $+1$) wavelet-transformed V_m (Fig. 3A). Phase differences between V_m and LFPs were computed with a time resolution of 1 ms along 400-ms time windows centered at UP state onsets. The window length was selected on the basis of previous work correlating cortical LFP, cortical multiunit activity, and striatal transitions between the UP and DOWN states (11). The mean direction of the circular distribution of these 400 phase differences was taken as the phase difference during the transition (PDT). This provided, for each UP state onset, three PDTs, one per LFP, and one average PDT. Analogous methods were used to estimate PDTs during transitions to the DOWN state (see *SI Text* for more details). In some cases, an LFP recording was discarded because electrode misplacement resulted in traces with no prominent slow waves.

Statistics. Data are expressed as mean \pm SEM, unless stated otherwise. Partial least-squares multivariate statistics was implemented as described in *SI Text*. Further comparisons were made with repeated-measures ANOVAs (Holm Sidak post hoc test), one way ANOVAs, or Kruskal–Wallis ANOVA for ranks, as appropriate. The statistical significance of a linear regression was measured from its ANOVA.

ACKNOWLEDGMENTS. We thank the editor and reviewers for valuable comments on the manuscript. This work was supported by National Institutes of Health Research Grant R03 TW6282 (to P.O.) funded by the Fogarty International Center and the National Institute on Mental Health; Secretaría de Ciencia, Tecnología e Innovación Productiva, Fondo para la Investigación Científica y Tecnológica (Argentina; PICT 05-11012 and 26323; PME2003-29), Universidad de Buenos Aires (UBACYT M056), and Consejo Nacional de Investigaciones Científicas y Técnicas (Argentina; PIP5890).

1. Steriade M, McCormick DA, Sejnowski TJ (1993) Thalamocortical oscillations in the sleeping and aroused brain. *Science* 262:679–685.
2. Steriade M, Timofeev I, Grenier F (2001) Natural waking and sleep states: A view from inside neocortical neurons. *J Neurophysiol* 85:1969–1985.
3. Crochet S, Petersen CC (2006) Correlating whisker behavior with membrane potential in barrel cortex of awake mice. *Nat Neurosci* 9:608–610.
4. Ferezou I, Haiss F, Gentet LJ, Aronoff R, Weber B, Petersen CC (2007) Spatiotemporal dynamics of cortical sensorimotor integration in behaving mice. *Neuron* 56:907–923.
5. Destexhe A, Hughes SW, Rudolph M, Crunelli V (2007) Are corticothalamic ‘up’ states fragments of wakefulness? *Trends Neurosci* 30:334–342.
6. Buzsáki G, Draguhn A (2004) Neuronal oscillations in cortical networks. *Science* 304:1926–1929.
7. Charpier S, Mahon S, Deniau JM (1999) *In vivo* induction of striatal long-term potentiation by low-frequency stimulation of the cerebral cortex. *Neuroscience* 91:1209–1222.
8. Goto Y, O’Donnell P (2001b) Synchronous activity in the hippocampus and nucleus accumbens *in vivo*. *J Neurosci* 21:RC131.
9. Kasanetz F, Riquelme LA, Murer MG (2002) Disruption of the two-state membrane potential of striatal neurons during cortical desynchronization in anaesthetised rats. *J Physiol* 543:577–589.
10. Mahon S, *et al.* (2006) Distinct patterns of striatal medium spiny neuron activity during the natural sleep–wake cycle. *J Neurosci* 26:12587–12595.
11. Kasanetz F, Riquelme LA, O’Donnell P, Murer MG (2006) Turning off cortical ensembles stops striatal UP states and elicits phase perturbations in cortical and striatal slow oscillations in rat *in vivo*. *J Physiol* 577:97–113.
12. Pennartz CM, *et al.* (2004) The ventral striatum in off-line processing: ensemble reactivation during sleep and modulation by hippocampal ripples. *J Neurosci* 24:6446–6456.
13. Ribeiro S, *et al.* (2004) Long-lasting novelty-induced neuronal reverberation during slow-wave sleep in multiple forebrain areas. *PLoS Biol* 2:E24.

14. Alexander GE, Crutcher MD, DeLong MR (1990) Basal ganglia-thalamocortical circuits: Parallel substrates for motor, oculomotor, "prefrontal" and "limbic" functions. *Prog Brain Res* 85:119–146.
15. Middleton FA, Strick PL (2000) Basal ganglia and cerebellar loops: Motor and cognitive circuits. *Brain Res Brain Res Rev* 31:236–250.
16. Zheng T, Wilson CJ (2002) Corticostriatal combinatorics: the implications of corticostriatal axonal arborizations. *J Neurophysiol* 87:1007–1017.
17. Haber SN, Fudge JL, McFarland NR (2000) Striatonigrostriatal pathways in primates form an ascending spiral from the shell to the dorsolateral striatum. *J Neurosci* 20:2369–2382.
18. Haber SN (2003) The primate basal ganglia: parallel and integrative networks. *J Chem Neuroanat* 26:317–330.
19. Haber SN, Kim KS, Maily P, Calzavara R (2006) Reward-related cortical inputs define a large striatal region in primates that interface with associative cortical connections, providing a substrate for incentive-based learning. *J Neurosci* 26:8368–8376.
20. Voorn P, Vanderschuren LJ, Groenewegen HJ, Robbins TW, Pennartz CM (2004) Putting a spin on the dorsal-ventral divide of the striatum. *Trends Neurosci* 27:468–474.
21. McGeorge AJ, Faull RL (1989) The organization of the projection from the cerebral cortex to the striatum in the rat. *Neuroscience* 29:503–537.
22. Berendse HW, Galis-de Graaf Y, Groenewegen HJ (1992) Topographical organization and relationship with ventral striatal compartments of prefrontal corticostriatal projections in the rat. *J Comp Neurol* 316:314–347.
23. Ebrahimi A, Pochet R, Roger M (1992) Topographical organization of the projections from physiologically identified areas of the motor cortex to the striatum in the rat. *Neurosci Res* 14:39–60.
24. Wright AK, Norrie L, Ingham CA, Hutton EA, Arbuthnott GW (1999) Double anterograde tracing of outputs from adjacent "barrel columns" of rat somatosensory cortex. Neostriatal projection patterns and terminal ultrastructure. *Neuroscience* 88:119–133.
26. Gervasoni D, et al. (2004) Global forebrain dynamics predict rat behavioral states and their transitions. *J Neurosci* 24:11137–11147.
27. Massimini M, Huber R, Ferrarelli F, Hill S, Tononi G (2004) The sleep slow oscillation as a traveling wave. *J Neurosci* 24:6862–6870.
28. Volgushev M, Chauvette S, Mukovski M, Timofeev I (2006) Precise long-range synchronization of activity and silence in neocortical neurons during slow-wave oscillations. *J Neurosci* 26:5665–5672.
29. Flaherty AW, Graybiel AM (1993) Two input systems for body representations in the primate striatal matrix: Experimental evidence in the squirrel monkey. *J Neurosci* 13:1120–1137.
30. West MO, et al. (1990) A region in the dorsolateral striatum of the rat exhibiting single-unit correlations with specific locomotor limb movements. *J Neurophysiol* 64:1233–1246.
31. Yeterian EH, Van Hoesen GW (1978) Cortico-striate projections in the rhesus monkey: the organization of certain cortico-caudate connections. *Brain Res* 139:43–63.
32. Selemon LD, Goldman-Rakic PS (1985) Longitudinal topography and interdigitation of corticostriatal projections in the rhesus monkey. *J Neurosci* 5:776–794.
33. Reep RL, Cheatwood JL, Corwin JV (2003) The associative striatum: Organization of cortical projections to the dorsocentral striatum in rats. *J Comp Neurol* 467:271–292.
34. Chang JY, Chen L, Luo F, Shi LH, Woodward DJ (2002) Neuronal responses in the frontal cortico-basal ganglia system during delayed matching-to-sample task: ensemble recording in freely moving rats. *Exp Brain Res* 142:67–80.
35. Fujii N, Graybiel AM (2005) Time-varying covariance of neural activities recorded in striatum and frontal cortex as monkeys perform sequential-saccade tasks. *Proc Natl Acad Sci USA* 102:9032–9037.
36. Pasupathy A, Miller EK (2005) Different time courses of learning-related activity in the prefrontal cortex and striatum. *Nature* 433:873–876.
37. Ding L, Hikosaka O (2006) Comparison of reward modulation in the frontal eye field and caudate of the macaque. *J Neurosci* 26:6695–6703.
38. Schultz W, Romo R (1992) Role of primate basal ganglia and frontal cortex in the internal generation of movements. I. Preparatory activity in the anterior striatum. *Exp Brain Res* 91:363–384.
39. Merchant H, Zainos A, Hernandez A, Salinas E, Romo R (1997) Functional properties of primate putamen neurons during the categorization of tactile stimuli. *J Neurophysiol* 77:1132–1154.
40. Hollerman JR, Tremblay L, Schultz W (1998) Influence of reward expectation on behavior-related neuronal activity in primate striatum. *J Neurophysiol* 80:947–963.
41. Kawagoe R, Takikawa Y, Hikosaka O (1998) Expectation of reward modulates cognitive signals in the basal ganglia. *Nat Neurosci* 1:411–416.
42. Costa RM, Cohen D, Nicolelis MA (2004) Differential corticostriatal plasticity during fast and slow motor skill learning in mice. *Curr Biol* 14:1124–1134.
43. Barnes TD, et al. (2005) Activity of striatal neurons reflects dynamic encoding and recoding of procedural memories. *Nature* 437:1158–1161.
44. Stern EA, Jaeger D, Wilson CJ (1998) Membrane potential synchrony of simultaneously recorded striatal spiny neurons *in vivo*. *Nature* 394:475–478.
45. Le Van Quyen M, Bragin A (2007) Analysis of dynamic brain oscillations: Methodological advances. *Trends Neurosci* 30:365–373.
46. Isomura Y, et al. (2006) Integration and segregation of activity in entorhinal-hippocampal subregions by neocortical slow oscillations. *Neuron* 52:871–882.
47. Hahn TT, Sakmann B, Mehta MR (2007) Differential responses of hippocampal subfields to cortical up-down states. *Proc Natl Acad Sci USA* 104:5169–5174.
48. Huber R, Ghilardi MF, Massimini M, Tononi G (2004) Local sleep and learning. *Nature* 430:78–81.
49. Magill PJ, et al. (2006) Changes in functional connectivity within the rat striatopallidal axis during global brain activation *in vivo*. *J Neurosci* 26:6318–6329.
50. Paxinos W (1997) *The Rat Brain in Stereotaxic Coordinates* (Academic, London), 3rd Ed.
51. McIntosh AR, Bookstein FL, Haxby JV, Grady CL (1996) Spatial pattern analysis of functional brain images using partial least squares. *NeuroImage* 3:143–157.